



Gray, D. and Le Kernec, J. (2018) Structural Antennas for 3cm Radar Onboard Multi-Rotor UAV. In: RADAR 2017: International Conference on Radar Systems, Belfast, UK, 23-26 Oct 2017, ISBN 9781785616730 (doi:[10.1049/cp.2017.0394](https://doi.org/10.1049/cp.2017.0394))

This is the author's final accepted version.

There may be differences between this version and the published version. You are advised to consult the publisher's version if you wish to cite from it.

<http://eprints.gla.ac.uk/140846/>

Deposited on: 14 June 2018

Enlighten – Research publications by members of the University of Glasgow
<http://eprints.gla.ac.uk>

Structural antennas for 3cm radar onboard multi-rotor UAV

D. Gray*, J. Le Kernec †

*XJTLU, China; derek.gray@xjtlu.edu.cn, †University of Glasgow, Scotland; julien.lekernec@glasgow.ac.uk

Keywords: slotted waveguide antennas, UAV.

Abstract

A series of 3cm amateur band radar antennas suitable for installation on a cinematic grade multi-rotor UAV were considered. A wideband open waveguide mouth antenna was developed that can be made from the existing arms of a multi-rotor UAV without any increase in weight for side-looking wall detection ranging radar. For downward looking radio altimeter, cutting slots in the arms to form slotted waveguide antennas was shown in simulation to be possible both in terms of covering the entire 3cm band from 10 to 10.5 GHz and without overly weakening the arms as structural members.

1 Introduction

Cinematic grade multi-rotor unmanned aerial vehicles (UAVs) are self-stabilizing flying platforms capable of hovering or low speed flight for periods of up to 40 minutes while carrying up to 4kg payloads, Figure 1. Consequently these UAVs are used for high quality photography for real estate and film. To date, these small UAVs have not been used for radio frequency applications, possibly due to the limited endurance. However, in an educational context where restricted flight time is not an operational impediment, these UAVs are attractive for student projects on radio frequency sensing and radar; students are engaged by being able to interact with an actual UAV (organize field trials and conduct flights) and likewise find the opportunity to work on a system to be integrated with the UAV exciting. Commercially available small mass X-band and 24 GHz FMCW radar units [1] make radar and machine vision projects possible for undergraduate and MSc project students. Also, single chip GaAs 24 GHz FMCW radar are in the market [2], as are GaAs component chips for X-band [3], enabling lower weight in-house custom radar design, fabrication and testing projects for students.

The majority of work to date has focused on initial antenna design and mechanical testing [4]. Related student projects investigating the viability of onboard processing of SAR imagery for machine vision [5] gave promising results. Likewise, legacy projects on Software Defined Radar are expected to be applicable to the side-looking radar for networking neighbouring UAVs [6]. Future projects will be designed under the assumption that fully autonomous flight will be required for flying multi-rotor UAVs in the most densely populated, 20 to 30 storey high rise urban environments for building exterior inspection, post-fire building interior/exterior inspection, first responders and environmental/pollution monitoring. Crucial to flight amongst

high rise buildings is the availability of dependable sensors to accurately position the multirotor UAV relative to the ground below and the nearest high rise building walls. As GPS suffers multipath and is easily jammed and GPS data for high rise apartment buildings will not always be available, Navigation by GPS and on-board inertial sensors for fully autonomous flight amongst high rise buildings is not considered to be feasible. Ultrasonic and passive/active infrared sensors are expected to be the primary sensors under clear flying conditions, but will be adversely affected by smog, smoke, fog, light rain, dust, wind and vortices around high rise buildings. Radar as secondary sensors will provide lesser ranging accuracy but with higher dependability in all but the most extreme weather conditions in which the UAV could not fly in any case.

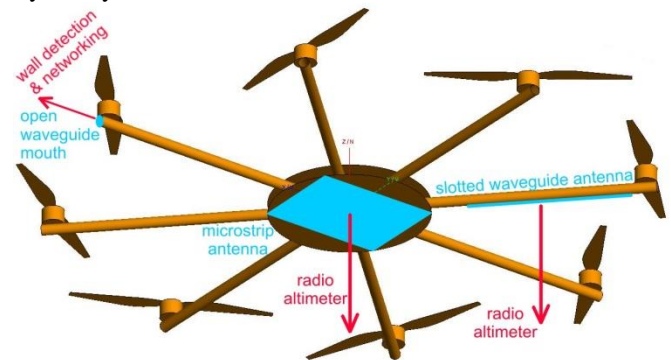


Figure 1: Antenna positioning onboard a 1.2metre diameter cinematic grade oct-rotor UAV.

The 24 GHz ISM band offers 1% fractional bandwidth across 24.00 to 24.25 GHz. Compared to X-band, the 24 GHz ISM band has the advantages of lower mass for high gain antennas and availability of single chip ranging radar [2], but requires higher accuracy (higher cost) for circuit board and antenna manufacturing. Advantages of the 3 cm amateur band are a wider 5% fractional bandwidth from 10.0 to 10.5 GHz and less stringent accuracy requirements for circuit boards and antennas.

The now discontinued Droidworx Skyjib 8 oct-rotor had a diameter of approximately 1.2 m, endurance of 40 minutes and maximum payload of 4kg, and is taken as a representative UAV design for this work (see Figure 1). The structural components were made of carbon fibre reinforced plastic (CFRP) which is a particulate hazard when drilled or machined; 6063 aluminium will be used instead of CFRP for an in-house built UAV. The central hub had a diameter of about 300 mm, and this downward facing surface is an ideal location to attach a microstrip patch array antenna for radio altimeter as that face is not obstructed by any attachments and is close to the controller and other electronics as shown in

Figure 1. The only potential problem with the underside of the central hub is possible interaction with the landing gear, which will be considered in the future patch array design. As the cross-section of the 540mm long circular tube CFRP arms were approximately the same dimensions as WR-90 waveguide, there is the unique opportunity to use the arms as structurally integrated end fire waveguide antennas for side-looking radar and as slotted waveguides for downward-looking radio altimeter without weight penalty causing reduced flight time as shown in Figure 1 [4]. A readily available 6063 aluminium rectangular tube with wall thickness of 1.2mm and inner dimensions of 22.6 by 9.6mm (cut-off frequency of 6.63 GHz) has been used to date. Such a hollow rectangular beam can either be orientated narrow wall or broad wall facing downward. Simulation of 500mm long 6063 aluminium rectangular tubes in COMSOL™ as cantilevers showed that von Mises stresses along the centre line of the upper face were approximately half and the overall deformation was about a third for narrow wall facing downward compared to broad wall facing downward as shown in Figure 2; therefore narrow wall facing downward was used for antenna design in this case.

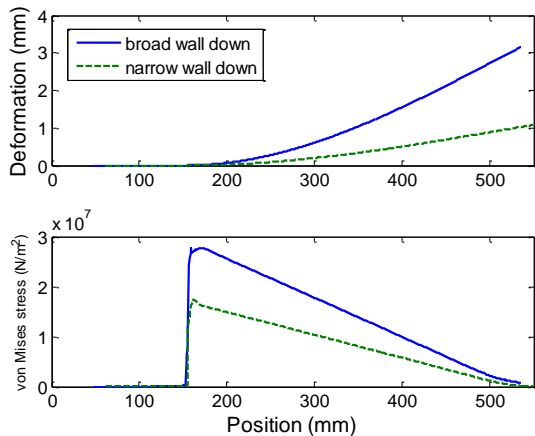


Figure 2: Deformation and von Mises stress along the centre line of the upward facing wall of 540mm long rectangular tubes with 3kg loading at outer end from COMSOL™.

The high risk part of this series of university student projects is the design, construction and bench top testing of the structurally integrated waveguide antennas. In this paper, initial antennas and ranging results are presented.

2 Side-looking end fire antennas

The 540mm long rectangular tube arm of the multi-rotor UAV will act as a low-loss transmission line at X-band, which allows for placement of a radar unit at the centre of the UAV at the inner end of the tube while the antenna is at the other end under a motor/propeller unit. Such an antenna should be readily built by hand by students, and thus requires a minimal number of parts and welds. One of the parabolic reflector feeds trialled in the early 1940s was clam shell like extensions of the broad walls. Here, the narrow walls were cut away to leave a half elliptical section of the broad wall, Figure 3. The long axis of the half elliptical section was 18.5 mm for all 3 units manufactured by hand.

For all 3 antennas, $S_{11} \leq -15$ dB across the amateur band, Figure 4. The repeatability of the 2 longer waveguide antennas was good. The only difference between the 2 long and the 1 short waveguide antenna was the length of the waveguide section, which caused a difference in the resonances.



Figure 3: Photographs of prototype end fire antennas; half ellipse length was 18.5mm long on all 3 antennas.

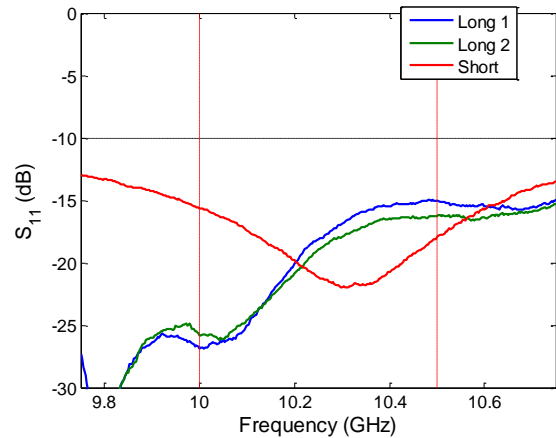


Figure 4: Measured S_{11} of end fire antennas shown in Figure 3; change in waveguide length changed resonances.

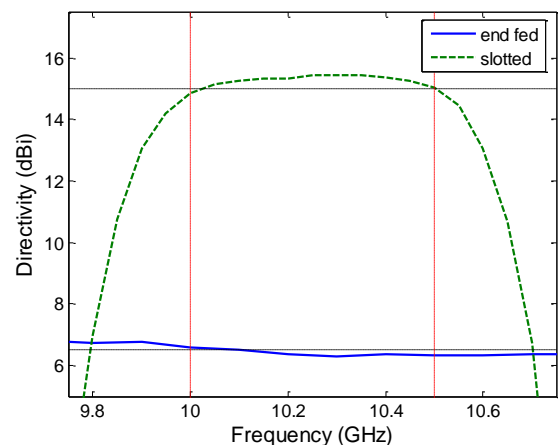


Figure 5: Typical Directivity performance of an end fire antenna and inclined-slot 10-slot slotted waveguide antenna; from FEKO™.

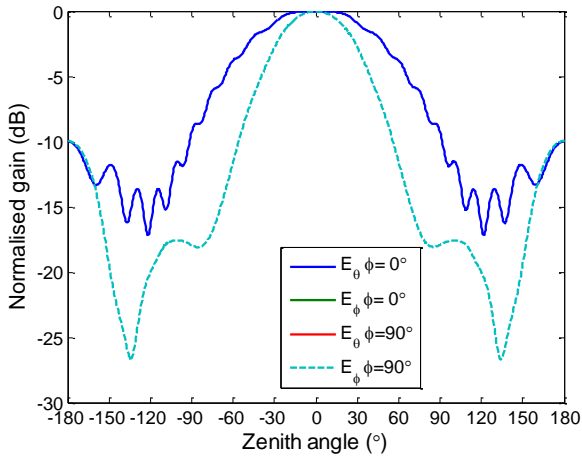


Figure 6: Typical linearly polarised radiation patterns of end fire antennas at 10.25 GHz; from FEKO™, cross-polarised components were below -30 dB.



Figure 7: Photograph of bistatic (quasi-monostatic) ranging radar measurement in a 17 m corridor section; end fire antennas in foreground, aluminium plate target at 5 m, corridor end wall with window at 17 m.

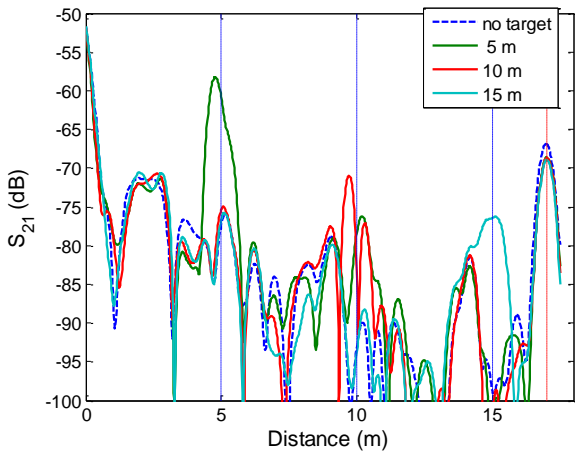


Figure 8: Measured range results in a 17 m corridor section, with 300 x 400 mm aluminium flat plate target at different positions: 5, 10 and 15 m.

In simulation, the antennas gave a close to flat Directivity response of 6.5dBi across 10 to 10.5 GHz, Figure 5 (blue line end fed); making these waveguide antennas a viable alternative to single microstrip patch antennas which will require heavy support cabling for an equivalent installation. The 3dB beamwidth in the H-plane was 62°, and varied from 100° to 110° in the E-plane due to ripple caused by TM standing waves on the outside of the waveguide, Figure 6. These standing waves are the likely cause of the S_{11} resonance shifts with waveguide length below $S_{11} \leq -15$ dB noted above. An initial bistatic (quasi-monostatic) ranging experiment was conducted at the end of a corridor using 2 end fire antennas and an Agilent 5230 PNA with Option 010 for Time Domain Analysis [7]. The antennas were 13 cm apart, 122 cm above the floor and 17 m from the wall at the end of the corridor. A 300 x 400 mm aluminium flat plate was moved to 5, 10 and 15 m from the antennas, giving detectable returns at those positions, Figure 8. The return from the wall at 17 m at the end of the corridor was seen in all measurements, showing that accurate ranging measurements could be made of all reflectors in the scene under observation.

3 Downward-looking Z-slot slotted waveguide antennas

As the rectangular tube arms of the oct-rotor UAV are to be orientated narrow walls up/down, inclined shunt slotted waveguides are the obvious antenna choice. These antennas will give a linearly polarised fan beam suitable for radio altimeter on a multi-rotor UAV [8]. Sets of 10 off 20° inclined slots were cut in 280mm lengths of the same aluminium tubing as used for the end fire antennas, Figure 9. Rough shaping was done with a hand saw, with small files used for finishing.

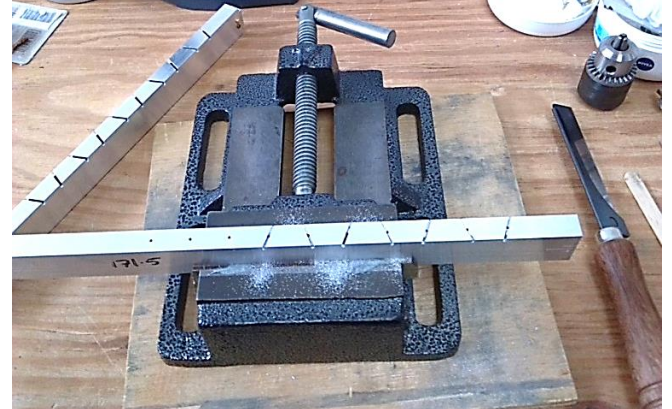


Figure 9: Manufacture of narrow wall inclined-slot 10-slot slotted waveguide antennas from 6063 aluminium tubing.

As for the end fire antennas, a pair of slotted waveguides were required for the ranging measurements using the PNA with Option 010. Despite being cut by hand, the S_{11} of the 2 antennas were close to identical as shown in Figure 10. Both antennas gave $S_{11} \leq -10$ dB across 10 to 10.5 GHz, as required. In contrast to the FEKO™ simulation, both antennas had a double resonance. The cause of the double resonance will be investigated in the future. In simulation, the slotted waveguide

antennas gave 9 dB higher directivity than the end fire antennas, Figure 5.

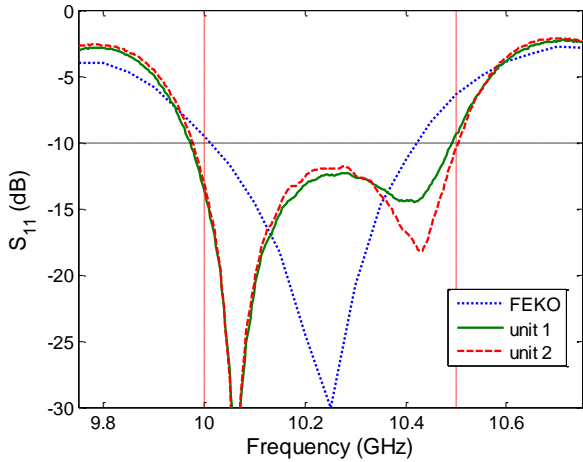


Figure 10: Measured S_{11} of narrow wall inclined-slot 10-slot slotted waveguide antenna at 10.25 GHz.

The fan beam of the inclined-slot 10-slot slotted waveguide antenna is perpendicular to the axis of the rectangular tube, which will partially compensate for the UAV rolling in that plane during manoeuvring or hovering against wind; the H-plane 3dB beamwidth was 91.5° , Figure 11. In the E-plane, along the tube axis, the beamwidth was 8° , with a first side lobe level indicating successful uniform aperture illumination (-13dB below peak). The E-plane cross-polarised peaks appeared as distinct lobes at $\pm 49^\circ$ which are -11.0dB below peak, which is considered inordinately high and a disadvantage of this antenna type.

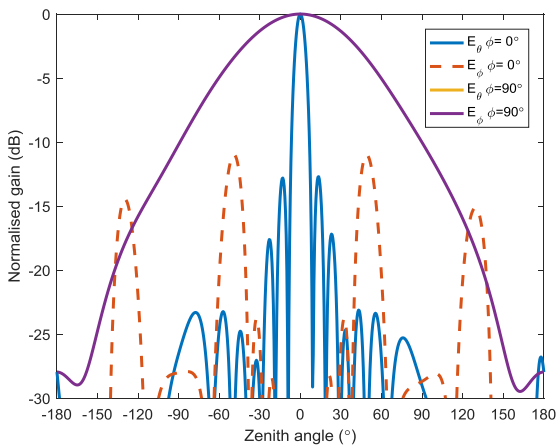


Figure 11: Radiation patterns of narrow wall inclined-slot 10-slot slotted waveguide antenna at 10.25 GHz; from FEKOTM.

The slotted waveguide antennas were used for an initial in-door ranging experiment identical to what was undertaken with the end fire antennas above; the antennas were held 130mm apart with a foam spacer, were vertically polarised, and mounted on the same trolley with the PNA 17 m from the end of the corridor, Figures 12 and 13. Superficially, the ranging results appear identical, Figures 8 and 13. On closer examination,

return from the corridor end wall using the slotted waveguide antennas was 7 dB higher and 10dB higher for the blue wall reflection, been close to the directivity difference of 8.5 dB. This result was sufficient to warrant proceeding to outdoor tests.

There was an apparent increased error in the positioning of the flat aluminium plate; the plate was measured as been at 4.5 m instead of 5 m, and there was a 1metre error for the other 2 positions.

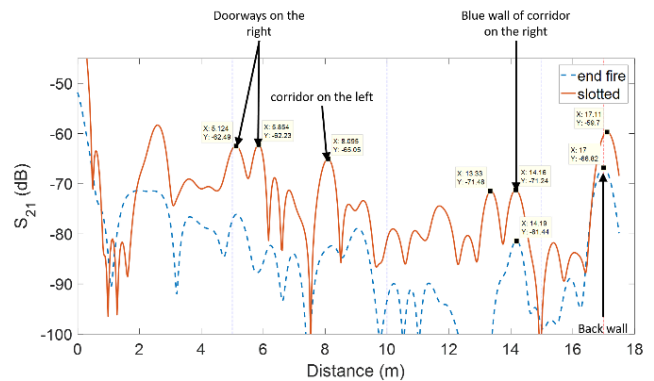


Figure 11: measurements of the experimental ground without targets.

After a closer observation of the scene Figure 7 and 12 and understanding the beam pattern of the antenna placed as such would result in a horizontal fan beam and a narrow beam vertically, the doorways observed in the right-hand side constitute corner reflectors around 5 m accounting for the error then the large errors observed at 10 and 15 m are caused by the corridors on the left and right as indicated in Figure 11 that affect the positioning accuracy. However, the end wall of the corridor at 17m is detected at the right distance 17.1 m for the slotted antenna and 17 m for the end fire antenna. This means that to appropriately test the ranging accuracy the next stage of ground testing will be done outdoors between building tops to avoid clutter affecting the position of the reflector.

The arms of the proposed in-house built oct-rotor UAV are critical structural parts. Drilling or cutting any holes or slots will weaken the arms, and increase the risk of mechanical failure during flight. As an initial attempt to gauge the degree to which the inclined slots cutting the corners of the rectangular tube will weaken it, a series of COMSOLTM simulations were undertaken [4].

Without conducting actual mean time to failure measurements on the 6063 aluminium tubes perforated with slots this quantity remains unknown, however long term metal fatigue will be influenced by deformation and peak von Mises stress. The COMSOLTM rectangular tube cantilever model, used for Figure 2, was modified to represent a conventional inclined 10 slot and a 10 Z-slot slotted waveguide antennas, and rerun with 3kg loading on the tube ends as an extreme loading case [4]. The tube with inclined slots suffered twice the deformation at the tube outer end and 30% higher von Mises stress on the centre line of the upward facing narrow wall at the anchor point

on the edge of the central hub compared to the plain unslotted tube, Figure 14.

Dog-bone and H shaped slots are historical alternatives which fitted entirely within a narrow wall and did not require cutting the corners of the rectangular waveguide [8]. Distorting the H shaped slots into Z shapes has produced satisfactory 10-slot antennas [4], Figure 15. In contrast to the inclined slot slotted waveguide antennas, the Z-slot gave comparable deformation and von Mises stress results to the plain tube, Figure 14.



Figure 12: Photograph of bistatic (quasi-monostatic) ranging radar measurement in a 17 m corridor section; inclined-slot 10-slot slotted waveguide antennas in foreground, aluminium plate target at 5 m, corridor end wall with window at 17 m.

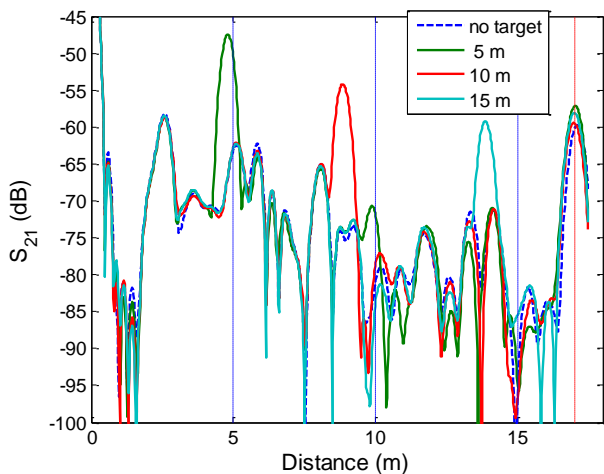


Figure 13: Measured range results in a 17 m corridor section, with 300 x 400 mm aluminium flat plate target at different positions: 5, 10 and 15 m.

A further worrying result from the inclined slots case was that the von Mises stress around the square corners of the broadwall ends of the inclined slots was greater than the tear strength of 6063 alloy aluminium, suggesting immediate tearing and structural failure. This will be investigated during cantilever test in the future.

Moving the sets of 10 slots outward away from the anchor point decreased the von Mises stress seen along the centre line of the upward facing non-slotted narrow wall. This, likewise, will be investigated during experimental work.

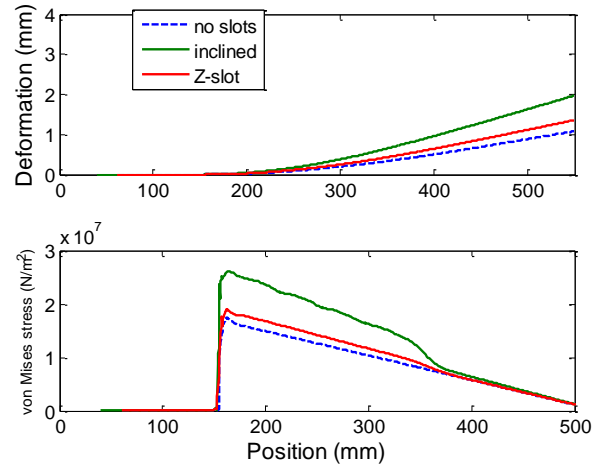


Figure 14: Deformation and von Mises stress along the centre line of the upward facing narrow wall of 540mm long rectangular slotted tubes (3 kg load); from COMSOL™.



Figure 15: A conventional copper WR-90 inclined edge slot antenna and a Z-slot aluminium tubing antenna.

A unique feature of the Z-slot slotted waveguide antennas in FEKO™ simulation was a double resonance, which if managed enables wide $S_{11} \leq -10$ dB bandwidth. A slot spacing of 19 mm was used here, and $S_{11} \leq -10$ dB was obtained across the 3cm amateur band, Figure 16. The Directivity was better than 15 dBi across the entire band, been 0.2dB higher than that from the inclined slot antenna.

The Z-slot slotted waveguide antenna produced a radiation pattern similar to that of the inclined slot antenna, having a fan beam perpendicular to the axis of the rectangular tube; the H-plane 3 dB beamwidth was 98° , Figure 17. In the E-plane, along the tube axis, the beamwidth was 8° , with a first side lobe level indicating successful uniform aperture illumination (-13dB below peak). As with conventional inclined slot slotted waveguide antennas, there are high cross-polarised lobes at $\pm 48^\circ$, but were -13.1 dB below peak, representing an improvement over the conventional inclined slot antennas.

The first Z-slot slotted waveguide antenna proved to be extremely laborious to manufacture, requiring some hundreds of 1.5 mm drill holes. The design has been refined by

increasing the width of the verticals of the H shaped to 3 mm [9]. Progress with manufacture and testing of the improved design will be reported during the presentation.

The COMSOL™ simulations were done by Mr. Q. Lan, while he was supported by the XJTLU 2014 Summer Undergraduate Research Fund program.

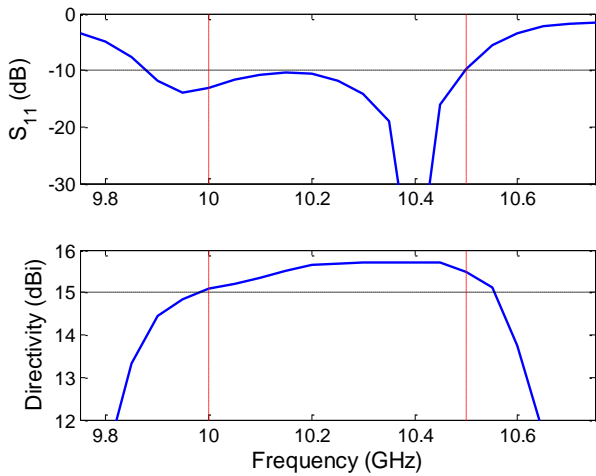


Figure 16: S_{11} and Directivity of 10 Z-slot slotted waveguide antenna; from FEKO™.

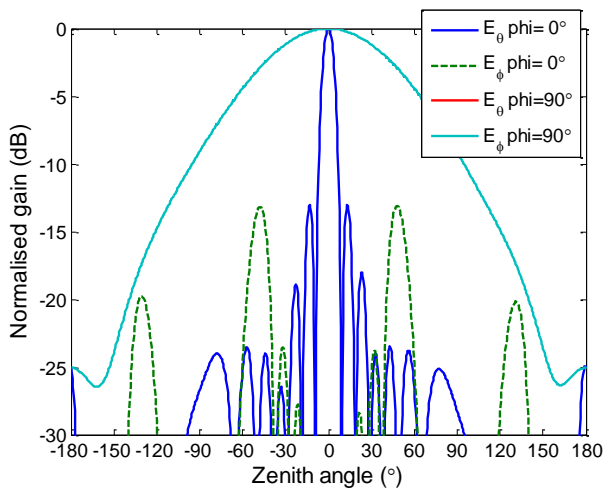


Figure 17: Radiation patterns of Z-slot 10 slotted waveguide antenna 10.25 GHz; from FEKO™.

4 Conclusions and Future work

Two classical waveguide antennas were successfully adapted to the 3cm Amateur band and for construction from low cost 6063 aluminium alloy extruded tubing, which would be used as the arms of an in-house built oct-rotor UAV. The initial antenna prototypes were made entirely by hand. Pairs of like antennas were used for an initial in-door “bench top” ranging experiment in a wide corridor. Although there were many false returns, the corridor end wall was clearly and accurately detected at 17 m, akin the operating altitude of the UAV. Having successfully gained ranging results for a ground surrogate, outdoor trials will be undertaken. Progress with the Z-slot slotted waveguide antenna manufacture and outdoor testing will be reported in the presentation.

Acknowledgements

References

- [1] *FMCW Radar Sensors: Applications notes*, Siivers IMA AB, (2011).
- [2] *BGT24MTR11 Silicon Germanium 24 GHz Transceiver MMIC*, Infineon Technologies AG, (2013).
- [3] *HMC530LP5 MMIC vco with half frequency output & divide by 4, 9.5 - 10.8 GHz*, Hittite Microwave Corporation, (2015).
- [4] Q. Lan, D. Gray, Y.-T. Chen & K. Sakakibara, “Width effects on electromagnetic and mechanical behaviour of Z-slotted waveguide array antennas”, *IEEE Antennas Propagat. Symp.*, (2015).
- [5] A. Melnikov, J. Le Kerneec & D. Gray, “A Case Implementation of a Spotlight Range Migration Algorithm on FPGA Platform,” *Int. Symp. Antennas Propagat.*, (2014).
- [6] J. Le Kerneec, D. Gray & O. Romain, “Empirical analysis of Chirp and Multitones performances with a UWB software defined radar: range, distance and Doppler,” *Asia-Pacific Conf. Antennas Propagat.*, (2014).
- [7] Time Domain Analysis Using a Network Analyzer, Application Note 1287-12, Agilent Technologies, May 2, 2012.
- [8] A.A. Oliner & R.G. Malech, “Radiating elements and mutual coupling,” in *Microwave scanning antennas*, R.C. Hansen, Ed., Academic Press Inc., **vol. 2**, (1966).
- [9] D. Gray, “Load bearing slotted waveguide antennas for radio altimeter,” *IEICE Technical Report*, Hiroshima Institute of Technology, January 2017.